Cluster Computing (2019) 22:S12179–S12191
https://doi.org/10.1007/s10586-017-1580-2

An automated and hybrid method for cyst segmentation in dental X-ray images

R. Karthika Devi[1] · A. Banumathi[2] · G. Ulaganathan[3]

Received: 7 October 2017 / Revised: 10 December 2017 / Accepted: 18 December 2017 / Published online: 5 February 2018

Abstract
The dental X-ray image has poor contrast and uneven exposure which results in the lack of reliable separation between various parts of teeth, which makes the segmentation of cyst very tedious. A unique hybrid automated technique has been proposed to detect and extract the cystic region using circularly symmetric isophote properties and fast marching method.The isophote curvature is the curve connecting the same intensity pixels. Each Isophote curvature line has an isocenter associated with it. Among them, the isocenter which is having a maximum response in the isophote center map to be concluded as the most likely estimate for locating the cystic region. This Maximum IsoCenter (MIC) is the seed point to the model-based segmentation of fast marching method. The fast marching algorithm (FMM) is like Dijkstra's algorithm, and it follows the shortest path from seed area, where the information flows outward only. It works systematically to make it fast, and it is a one-pass method because each point is touched only once mainly. This fast marching method extracts the cystic region boundary very effectively and efficiently. This two-stage hybrid method is an automated, robust, and fast method for solving the complex problem of cyst segmentation. The average execution time calculated is 2.8 s and the accuracy achieved is 95%. The performance outcomes show that the proposed segmentation technique has the high correlation with the manual method. Therefore, the combination of model-based and feature based segmentation of the dental X-ray images has great potential in diagnosis of dental diseases and plays a significant role in the development of automated systems. The automated segmentation computerizes or automates the diagnostic method so that huge number of patients can be monitored with the same assured accuracy. High-speed computers are helpful in attaining fast and precise results. To extend the patient care to remote areas, the faster communication is possible by computer networks

Keywords Computer aided detection · Dental X-ray images · Isophote curvature automated dental cyst detection · Fast marching method · Cyst boundary extraction

1 Introduction

In the field of dentistry, the digital dental X-ray analysis is more convenient and easier by automation of computer-aided diagnosis in the massive amount of database. A dental cyst is a major problem, which causes sudden pain in the affected region and starts reaching the jaw, gums, and face. Therefore, it is important to remove the cyst to stop the spreading of infection on any other parts of the mouth. Recently, computer-aided detection or diagnosis (CAD) has become an important research in digital dental X-rays. The Computer-aided diagnosis helps to improve the accuracy of diagnosis, measuring severity, automatic dental cyst detection, and speed up the operation of reading and interpretation of the medical image by the manual operator. The dental diagnosis will become easier using CAD-based digital dental X-ray because the hidden bone and teeth under cortical plate surface also well seen by dental practitioners during visual examinations. The main advantages of dental X-ray images are instant availability, radiation dose applied is very less, a possibility of image enhancement and reconstruction and make the dental X-ray analysis, more convenient by CAD [1].

✉ R. Karthika Devi
jayanidhaya@gmail.com

1 Department of Electronics and Communication Engineering, Sethu Institute of Technology, Pulloor, Virudhunagar, Tamilnadu, India

2 Department of ECE, Thiagarajar College of Engineering, Madurai, Tamilnadu, India

3 Department of Oral Surgery, CSI College of Dental Science & Research, Madurai, Tamilnadu, India

After the development of computer-aided diagnosis or detection, better diagnosing and decision-making become easier for the further treatment process by the dentist. Radiologists depend on computer-aided methods for early diagnosis effectively. There is no unique automated segmentation method to be applicable for all type of images. The image segmentation should be unique and more complex depending upon the domain of application. Digital dental X-rays have three views they are the panoramic view, periapical view, and bitewing view [2]. Among them, frequently used one is the periapical view which includes only a fewer teeth with their root and their bones in the surroundings.

These periapical views are handy and very useful in the detection of lesions like a bone loss by periodontal diseases and dental caries. The periodical dental X-rays are most widely used modality in dental imaging, and it is a very challenging work to make it fully automatic for computer-aided diagnosis and detection of dental diseases.

2 Dental X-ray image segmentation

The medical image segmentation can be classified as manual, semi-automatic, and automatic segmentation. Based on that classification, the Manual segmentation discusses the procedure whereby medical expert fragments and labels a medical image by hand. The Automatic segmentation mentions the method whereby segment boundaries are allotted automatically by the program. Semi-automatic segmentation states the process whereby that automatic segmentation is followed by manual examination and decides the segmented boundaries. The cyst segmentation also involves three types of segmentation. Here for manual segmentation, the live—wire algorithm by Chodorowski et al. [3].

With growing use of digital dental radiography and CBCT imaging for dental diagnosis, treatment, and clinical studies, it becomes necessary to use the computer to help radiological experts in disease diagnosis and planning of treatment. The reliable and consistent algorithms are in demand for the delineation of the region of interest (ROI). Then the cyst segmentation techniques are mainly classified into two main groups as semi-automatic or fully automatic.

The semi-automatic methods are mostly level set method [4], live wire [5,6], active contour [7]. All the semi-automatic methods are coming under the deformable models that are model-based techniques for region boundary delineation. They are using the surfaces or closed curves that deforming under some influence of internal or external forces. For delineating the object boundary, a surface or closed curve will first be positioned nearer to the desired object boundary. Then it is allowed to go through an iterative process called relaxation. The main advantages of this deformable models are, it can able to generate surfaces or closed curves from the desired images with the incorporation of smoothing factor constraint that gives robustness to the noise present and the spurious edges. The disadvantage of that method is, it requires manual interaction for placing initial model and selection of appropriate parameters.

The advantages of automated segmentation are, to computerize or automate the diagnostic method so that huge number of patients can be monitored with the same assured accuracy. High-speed computers are helpful in attaining fast and precise results. To extend the patient care to remote areas, the faster communication is possible by computer networks. From the survey, the fully automatic methods already proposed for segmentation of lesion in the dental X-rays are, model-based level set method [8],similarity-based region growing approach [5,9], histogram based thresholding approach [10], mask based template matching [11], texture-based segmentation [12]. The particle swarm optimization and adaptive threshold technique for liver cyst segmentation proposed in [13]. The MSER based segmentation for liver cyst segmentation proposed in [14].

From the above survey, there are some complications identified in the segmentation of dental cysts. They are

(1) Complicated teeth structure.
(2) The orientation of teeth is arbitrary.
(3) It is noisy due to sampling artifact.
(4) The contrast of the dental image is too low, and the uneven exposure makes the intensities of teeth, gums, and bones similar to visual cues.
(5) The absence of strong lines of separation between regions of interest makes complication in differentiating healthy and unhealthy structures. Therefore, it is unable to identify the edges of teeth, bone, and gums [4,8,10].
(6) The cysts can have different size and location so radiologist should carefully do the parameter initialization [5,10].

The human inspection offers only subjective information, which will vary from dentist to dentist and will not provide quantitative data for analysis. At the same time, even some early stage lesions will not be visible to the human eye. The traditional segmentation algorithms generate more false positive rates and prone to segmentation error. All of the problems mentioned above show the difficulties in implementing automated segmentation actually in the computer-aided diagnosis, and there is a necessity for very efficient and accurate automatic dental X-rays analysis. Figure 1 shows the jaw- bone cysts radicular and follicular cysts. The literature survey carried out for dental X-ray lesion segmentation shown in Table 1. It listed out the modality, view and the types of carious lesion, cyst, and plaque, the segmentation techniques like semi-automatic or fully automatic. Most of the techniques are automatic

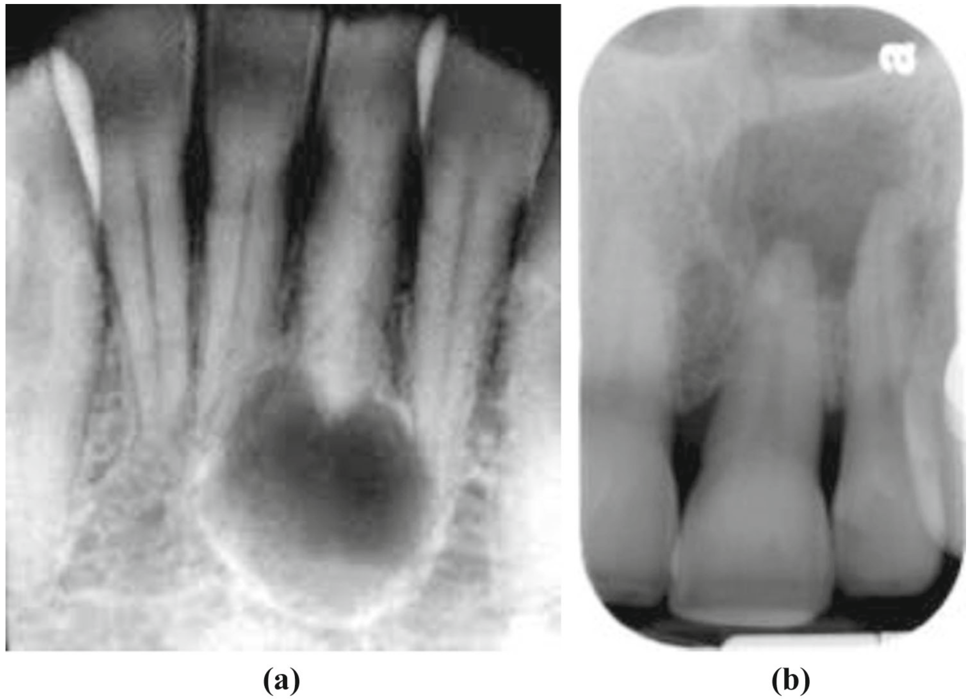

Fig. 1 Types of dental cyst. **a** Radicular cyst. **b** Follicular cyst

which reduces the manual intervention. The shortcomings in cyst segmentation addressed earlier will be overcome by the proposed a two-stage, the fully automated hybrid methodology using Isophote curvature with fast marching algorithm. The proposed method is a new fast, hybrid, and two-stage, automatic segmentation for cyst boundary extraction. The advantages attained by the proposed methodology are

(1) There is a strong line of separation between the cystic region and other parts of the teeth.
(2) It is fully automatic, so no parameter initialization required.
(3) The complicated cystic region also extracted.
(4) It extracts any type cyst, which is variable in size and location.
(5) This method eliminates the time consuming, laborious manual segmentation, and the need of trained radiologist.

3 Modeling the dental cyst as an isophote curvature

The Cyst is a capsule formed in the root of the tooth, which creates radicular inflammation in tooth membrane and causes infections. A dental cyst is a significant problem, which causes sudden pain in the affected region and starts reaching the jaw, gums, and face. Therefore, it is essential to remove the cyst and stop the spreading of infection on any other parts of the mouth. Based on the several factors that are location, causes, and shape, the dental cyst is, classified as the radicular and follicular cyst, which are mostly circular shown in Fig. 1. Figure 2 (a) shows the layers in the cyst [2].They are

1. Lumen (cavity) - yellowish cyst fluid.
2. Epithelial lining - thick irregular net like rings. There is no distinct basal cell layer.
3. Wall (capsule) - composition of collagenous fibrous connective tissue.

The isophote of an image looks like contour maps which are the lines drawn through the constant area of brightness. It is the most crucial geometric information of an image, which describes the connection of the surface points having the continuous contrast and intensity through curves, which are called as isophote or level lines shown in Fig. 2b. By comparing the cyst feature Fig. 2a with isophote feature Fig. 2b, the lumen and lining of cyst are the more prominent circular features in the cyst. They have constant gray value along the lumen and lining. Within the layers, the intensity will be nearly same. Therefore it will characterize the features of cyst using isophotes, which are the curves connecting the equal intensity points and the Isophotes does not intersect each other [15,16]. Therefore, Isophote represents the feature, which is having same gray value in the circular or semi-circular region of the cystic region. Valenti et al. [16] proposed a hybrid method for eye location in low-resolution images. They characterized the eye by its pattern, which is having radially symmetric brightness. Therefore, they use

Table 1 Survey on segmentation of lesion in dental X-ray images

S. No.	Author	Work type	Method	Year	Imaging modality/view/lesion
1.	Li et al. [4]	Semi-automatic	Level set	2007	X-ray/periapical/ gums lesion X-ray/periapical/gums lesion
2.	Lin et al. [8]	Automatic	Level set + labelling	2012	X-ray/periapical, gum lesion
3.	Birdal et al. [9]	Automatic	Wavelet transform, region growing	2015	X-ray/panoramic/root apical lesions
4.	Alazab et al. [5]	Automatic	Region growing	2009	X-ray/periapical/lesions and various dental caries
5.	Chodorowski et al. [3]	Semi-automatic	Livewire operation	2005	Oral Color image/oral leukoplakia and lichenoid reactions
6.	Hamarneh et al. [7]	Semi-automatic	Active contour	2000	Oral Color image/the oral lesion, leukoplakia, and lichenoid reactions
7.	Abdolali et al. [10]	Automatic	Thresholding	2016	CBCTpanoramic//various types of jaw cysts
8.	Banumathi et al. [11]	Automatic	Template matching	2009	X-ray/periapical/dental cyst
9.	Mikulka et al. [6]	Semi-automatic	Livewire	2013	X-ray/Panoramic/various types of jaw cysts
10.	Katsumata et al. [1]	Automatic	CAD	2014	X-ray/panoramic and CBCT/cyst
11.	Berdouses et al. [12]	Automatic	Intensity and texture based	2015	Color tooth photographic images/single or multiple tooth/caries

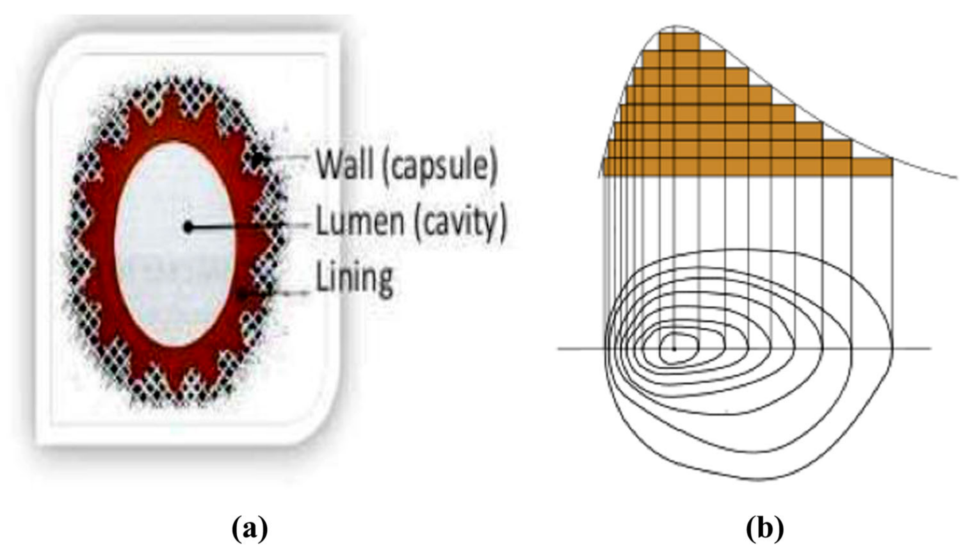

Fig. 2 Model of the dental cyst. **a** Layers of the dental cyst and **b** isophote contour lines with intensity map

Isophotes to represent the center of circular or semi-circular patterns. The isophotes are invariant to the changes of linear lighting and in-plane rotation. Like the eye, cyst also had radially symmetric brightness patterns. Mostly the follicular and radicular cyst is in a circular or semi-circular form shown Fig. 1. Therefore, we can adopt the isophotes to find the radially symmetric circular and semi-circular patterns in brightness. It is already measured and given that the follicular cysts are having the circularity of 0.807 ± 0.149 and radicular cysts having the circularity of 0.932 ± 0.086 [6]. Therefore, the Isophotes are used to locate the cyst and for seed selection in the cystic region of the digital dental X-ray images.

4 The proposed automated and hybrid model for dental cyst segmentation

Several image segmentation techniques were introduced to segment the dental cyst from the periapical X-ray image.

Table 1 gives the literature survey related to dental cyst segmentation. The segmentation can be classified as (i) model based (ii) feature based and (iii) hybrid methods. By the use of the global appearance, the advantages of model-based methods are very robust and accurate in detection, but the success depends only on the convergence of the model. The prior knowledge-based segmentation involves active shape and appearance models, active contours and deformable templates and level-set based methods. When considering, feature-based methods utilize distinguished properties (like symmetry) to detect objects from local image features (e.g., corners, edges, gradients), without the requirement of any learning model or model fitting. The feature-based methods can easily locate the object, even in a noisy surrounding. However, it may be incorrect and less stable than the model-based methods. The methods used for image segmentation are varied depending on the application, modality used, body region, and others. There is no single segmentation method can produce accurate, acceptable and automated results. By combining different segmentation methods, to make a hybrid framework can improve the performance of segmentation. By that, it can amplify the output performance and decrease the weakness of individual approaches. In the proposed methodology, model-based fast marching and feature based Isophote methods are combined to yield better results and make it fully automated in reducing the manual delineation by the manual operator in the large patient database.

The proposed hybrid method of cyst segmentation using isophote curvature and fast marching method shown in Fig. 3, which has two steps. They are

1. Seed point selection using maximum isocenter: the feature-based isophote curvature is used for the selection of initial seed point using maximum isocenter (MIC)
2. Cyst segmentation using Fast marching method: the model-based fast marching method (FMM) is used for dental cyst segmentation in the dental X-ray image.

4.1 Seed point selection using maximum isocenter (MIC)

The feature-based isophote curvature is used to extract seed location for the model based fast marching method. Here it is explained how the isophote curvature extracts the seed location in this section.

The differential invariants are fundamental in projective geometry, where the derivatives do not show many changes when the position and direction coordinate of the system are fully arbitrary, which makes it invariant to translation and rotation of the coordinate system. There are many methods to achieve this. One of the methods used in 2D is intrinsic geometry with gauge coordinates the example is curvature study. The local and intrinsic derivative coordinates used in

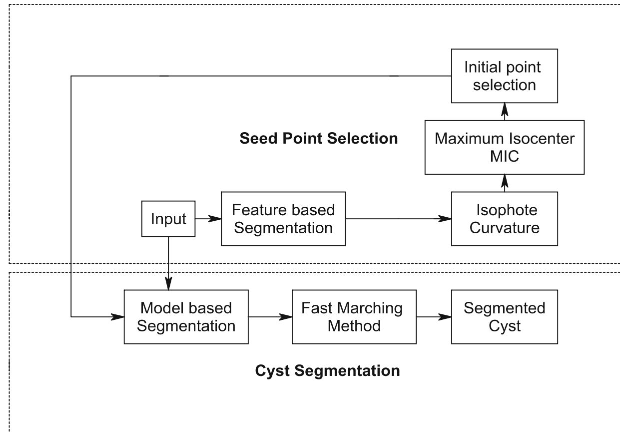

Fig. 3 Flowchart of proposed of the two-stage hybrid method

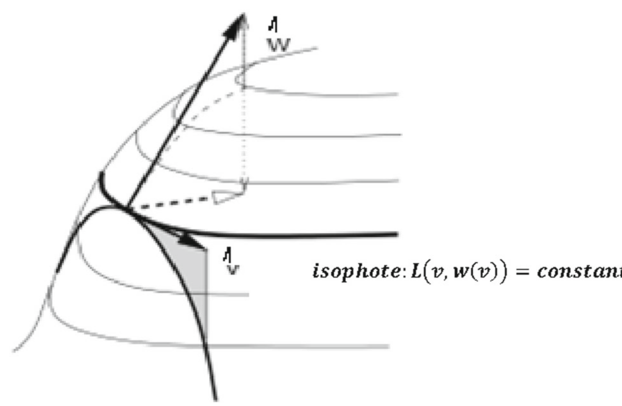

Fig. 4 Isophote curvature

the image for the Isophote description are called as Gauge coordinates shown Fig. 4. The full image is represented by the Isophotes. The duality in the system is, the Isophotes are calculated from the pixel and vice versa [15,16].

The local pair of unit vectors {v, w}, are the first order gauge frame in the image where v points are in Isophotes tangential direction and w in the gradient direction which is orthogonal to v. Therefore, every pixel in an image attached to the {v, w} local frame, which oriented differently and derivatives of v and w is invariant to translation and rotation where gradient magnitude is $\frac{\partial L}{\partial W} = L_x$ and $\frac{\partial L}{\partial V} \equiv 0$ that is there is no luminance change in the tangential direction of Isophote[16].

$$\hat{w} = \frac{\{L_x, L_y\}}{\sqrt{L_x^2 + L_y^2}}; \quad \hat{v} = \perp \hat{w} \tag{1}$$

$$w = \frac{1}{\sqrt{L_x^2 + L_y^2}} \begin{pmatrix} L_x \\ L_y \end{pmatrix} \quad v = \begin{pmatrix} 0 & 1 \\ -1 & 0 \end{pmatrix} \cdot w \tag{2}$$

The definition of isophote is $L(v, w(v)) = \text{constant}$ and differentiating isophote definition concerning v, we get

$$L_v + L_w w'(v) = 0\,;\; w'(v) = -\frac{L_v}{L_w} \tag{3}$$

From the condition of gauge $L_v = 0$ leads to $w'(v) = 0$. Again differentiating the isophote definition with respect tov we get

$$L_{vv} + 2L_{vw} w'(v) + L_{ww} w'(v)^2 + L_w w''(v) = 0 \tag{4}$$

Let $K = w''(v)$ and $w'(v) = 0$

The isophote curvature through L_w(edge strength) can be

$$K = -\frac{L_{vv}}{L_w} \tag{5}$$

Therefore the isophote curvature is defined as $w''(v)$, the change of the tangent vector $w'(v)$ in the v direction

$$K = -\frac{L_{vv}}{L_w} = -\frac{L_y^2 L_{xx} - 2L_x L_{xy} L_y + L_x^2 L_{yy}}{\sqrt[3/2]{\left(L_x^2 + L_y^2\right)}} \tag{6}$$

The L_x, L_y are the image first-order derivatives and L_{xx}, L_{xy}, L_{yy} are the second-order image derivatives of the luminance.

The lowest order variants calculated [16] given in the Table 2

The reciprocal of the curvature is the radius of isophote, given by

$$r = (K)^{-1} = -\left(\frac{L_y^2 L_{xx} - 2L_x L_{xy} L_y + L_x^2 L_{yy}}{\sqrt[\frac{3}{2}]{\left(L_x^2 + L_y^2\right)}}\right)^{-1} \tag{7}$$

Since the gradient is used for estimating the orientation, which is the direction of maximum luminance change. The curvature sign depends on the outer side intensity value of the curve. For the cyst brighter outer side, so the sign of the curvature is positive.

The displacement vector can be calculated by multiplication of the inverse of isophote curvature with the gradient $\frac{\{L_x, L_y\}}{L_w}$. To the estimated position of the centers, the $\{D_x, D_y\}$ are representing the displacement vectors.

$$\{D_x, D_y\} = \frac{\{L_x, L_y\}}{L_w}\left(-\frac{L_w}{L_{vv}}\right) = -\frac{\{L_x, L_y\}}{L_{vv}} \tag{8}$$

$$\{D_x, D_y\} = \frac{\{L_x, L_y\}\left(L_x^2 + L_y^2\right)}{L_x^2 L_{xx} + 2L_x L_{xy} L_y + L_x^2 L_{yy}} \tag{9}$$

The set of vectors is pointing towards the center of the circular structure. The collective vote of the displacement vectors is the rough estimation of the center, called as an accumulator. Since it is the rough estimation of the center, the Gaussian kernel is convolved with accumulator will results in the conversion of every cluster of votes into a sole estimate center. The contribution of every vector is nothing but weighing every pixel by its curvedness.

Table 2 Lowest order differential invariants

L_v	0
L_w	$\sqrt{L_x^2 + L_y^2}$
L_{vv}	$-\frac{L_y^2 L_{xx} - 2L_x L_{xy} L_y + L_x^2 L_{yy}}{L_x^2 + L_y^2}$
L_{vw}	$-\frac{L_x^2 L_{xy} + 2L_{xy} L_y^2 + L_x L_y (L_{xx} - L_{yy})}{L_x^2 + L_y^2}$
L_{ww}	$\frac{L_x^2 L_{xx} + 2L_x L_{xy} L_y + L_x^2 L_{yy}}{L_x^2 + L_y^2}$

4.1.1 The measure of curvedness

It is an image operator, which is used to measure, the deviation of region flatness and how much curved it is. The curvedness property measures, how much the shape curved. The curvedness is the rotational invariant gradient operator and measures the degree of steepness of the gradient.

$$\text{Curvedness} = \sqrt{L_{xx}^2 + 2L_{xy}^2 + L_{yy}^2} \tag{10}$$

This measure has lower responder on flat surface and object edges. It has the higher response in the places of maximal isophote density around the object edges. The curvedness is directly proportional to the density of the isophotes. The denser response of isophotes shows that they belong to the similar feature like edge so that they are pointing towards the same center. The higher curvedness is the result of denser isophote. The only isophotes, which are considered, has maximal curvedness mostly existing around the boundary of an object. Weighing the center voting by curvedness is advantageous over edge-based method, which avoids meaningless isophotes around edges. By summing up the votes, around the center of concentric Isophotes patterns, we will obtain the higher responses. The higher responses are called as isocenters or ICs. Among them, the maximum responsible isocenter is concluded as the most feasible estimate of locating the cyst region [16].

4.1.2 Automatic seed point selection in the cystic region using isophote curvature

The well-known layers of cyst lumen and lining are circular or semi-circular. Within the layers, the intensity of each pixel will be same approximately. With that prior knowledge, the proposed methodology uses maximum responsible isocen-

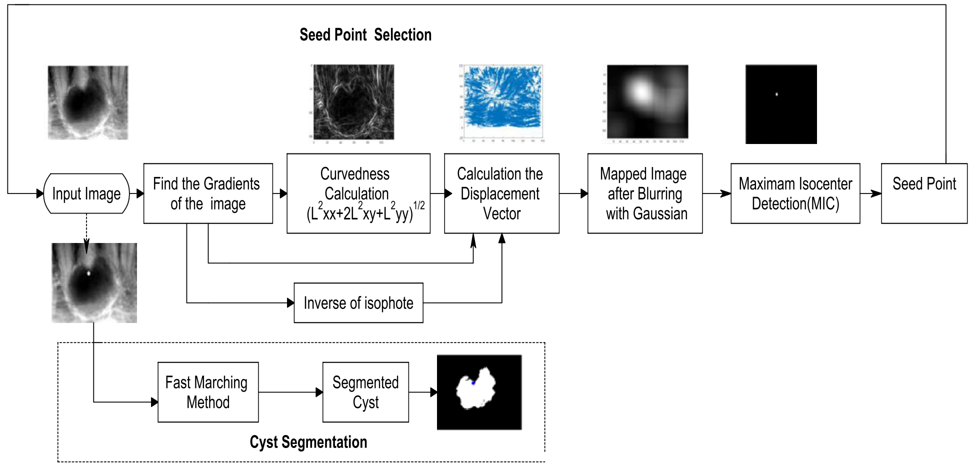

Fig. 5 Hybrid method-combination of isophote and fast marching method with intermediate results

ter [15,16] is used as seed in the cystic area. For locating the position of seed, the shape of the lumen and lining are considered as Isophote curves. The first order and the second order gradients are calculated for finding the Isophote curvature using Eq. (6). The displacement vector is found by multiplying the image gradient with the inverse of the Isophote curvature using Eq. (9).Each pixel is weighted differently by the curvedness which is calculated by Eq. (10) to locate the isocenter of the cyst and mapped on the accumulator. The detection of meaningful isocenters in the cystic region is found by the measure of curvedness. Among the isocenters, the maximum responsible isocenter (MIC) is used as the initial point or seed point for the fast marching method (FMM) to segment the cyst. The method is explained through the flowchart given in Fig. 5 with intermediate results.

4.2 Cyst segmentation using fast marching method

The model-based approach of fast marching method (FMM) is used for dental cyst extraction. The various steps involved in cyst extraction, shown in Fig. 5 and the detailed explanation given below.

4.2.1 The general fast marching method

The numerical method developed by Sethian (1996) for solving boundary value problems of Eikonal equation is fast marching equation [17].

$$F(x) \cdot |\nabla T(x)| = 1 \tag{11}$$

This numerical method describes the problem of curve evolution in the closed curve concerning the time T and with the speed of $F(x)$ in the normal direction on a curve at a point x. If the speed mentioned and at what time the contour passes a point x is acquired by finding the solution to the equation. The algorithm is like Dijkstra's algorithm, and it follows the path starting from seed point. So the information flows outward only. Also, this algorithm is a subset of level set methods. In general, the level set method is very slow.

The boundary formulated for all time to denote he expansion or contraction of boundary value problem. The effective, fast marching method obtained by making the interface moving in one direction. Always the interface propagated towards the next nearest value until it reaches the unknown node nearest to known node is called as fringe next.

The viscosity solution to the above Eikonal equation [17] given by

$$|\nabla u(x)| = F(x) \tag{12}$$

The construction of new points is developed by the envelope of the newer front, and the process is continued or repeated until the Eikonal solution is reached. The main idea is for solving exactly with starting with the known region. Also, the front is progressively going inside the curve or surface from the boundary in the domain shown in Fig. 6.

4.2.2 Approximation schemes for stationary formulation

For the boundary value formulation, for the multi dimension

$$|\nabla u(x, y, z)| = f(x, y, z) \tag{13}$$

Approximations for the multi dimension

$$|\nabla u| = \left[\sum\nolimits_{t=x,y,z} \mathrm{Max}(\mathrm{D}^{-t}_{\mathrm{ijk}}\mathrm{u}, 0)^2 + \mathrm{Min}(\mathrm{D}^{+t}_{\mathrm{ijk}}\mathrm{u}, 0)^2\right]^{1/2} = \mathrm{f}_{\mathrm{ijk}} \tag{14}$$

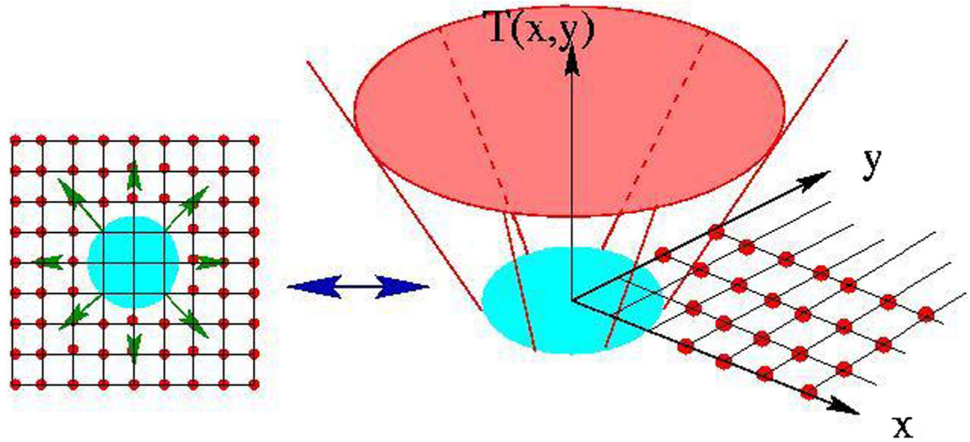

Fig. 6 Fast marching method as surface or front propagation

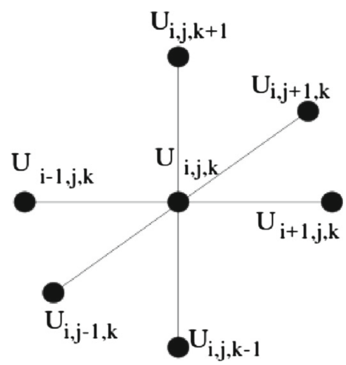

for i,,j,k=1 to mesh

Solve quadratic for $u_{i,j,k}^{itera+1}$given

$u_{i,j,k}^{itera}, u_{i+1,j,k}^{itera}, u_{i,j-1,k}^{itera}, u_{i,j+1,k}^{itera}, u_{i,j,k-1}^{itera}, u_{i,j,k+1}^{itera}$

end for

end for

Fig. 7 Updating the grid points

It can be rewritten for upwind scheme in a convenient way

$$\begin{bmatrix} \mathrm{Max}(D_{ijk}^{-x}u - D_{ijk}^{+x}u, 0)^2 + \\ \mathrm{Max}(D_{ijk}^{-y}u - D_{ijk}^{+y}u, 0)^2 + \\ \mathrm{Max}(D_{ijk}^{-z}u - D_{ijk}^{+z}u, 0)^2 \end{bmatrix}^{1/2} = f_{ijk} \tag{15}$$

where forward and where D^- and D^+ are the same forward and backward operators. The $_{Fij}$i is slowness at the grid point ijk shown in Fig. 7

4.2.3 FMM algorithm

The fast marching method relates the shortest path algorithm, named Dijkstra's method on a network. This Dijkstra's method is a globally known method used in the internet routing. The cost is an assignment of value to each node in the network to reach that point.

Initially, the solution to an Eikonal equation is, set of points called as Accepted points. It is the computed trial solution to Eq. 15 for the given value of 'u,' to get the accepted neighbor for an every not yet accepted points in the grid. Then tag all the points in the initial conditions as 'Accepted.' Then the points, which are one grid point away, are tagged as 'Considered' by solving the Eq. 15, then all other points are tagged as 'Far.'The steps in the FMM algorithm are

1. Start the loop with the trial seed point, i.e., maximum isocenter MIC, which tagged as 'Considered' point for the small value of u.
2. The Neighbors of trial points, which are not yet accepted, tagged as 'Considered.'
3. By solving the quadratic equation of the given Eq. 15, the value of 'u' recomputed at the all 'Considered' neighbors of the Trial point.
4. Add the trial point to 'Accepted' and eliminate from 'Considered.'
5. Return to starting loop until the 'Considered' set become empty.

It is a very effective algorithm, in ordering the path, in which the cost of the neighboring points is accepted. It works systematically to make it fast, and it is a one-pass method because every point is touched only once essentially. The critical point is, this technique lies in the fast method of locating the grid point in the narrow band with the smallest value for u. For the mesh with N points, the Computational efficiency of the fast marching method is O(N log N). The efficient method is devised using the min-heap structure which is similar to Dijkstra's method. N number of steps are used to touch the every mesh point where every step is O(log N) since the heap to be rearranged every time the values are changed. This fast marching method extracts the cystic

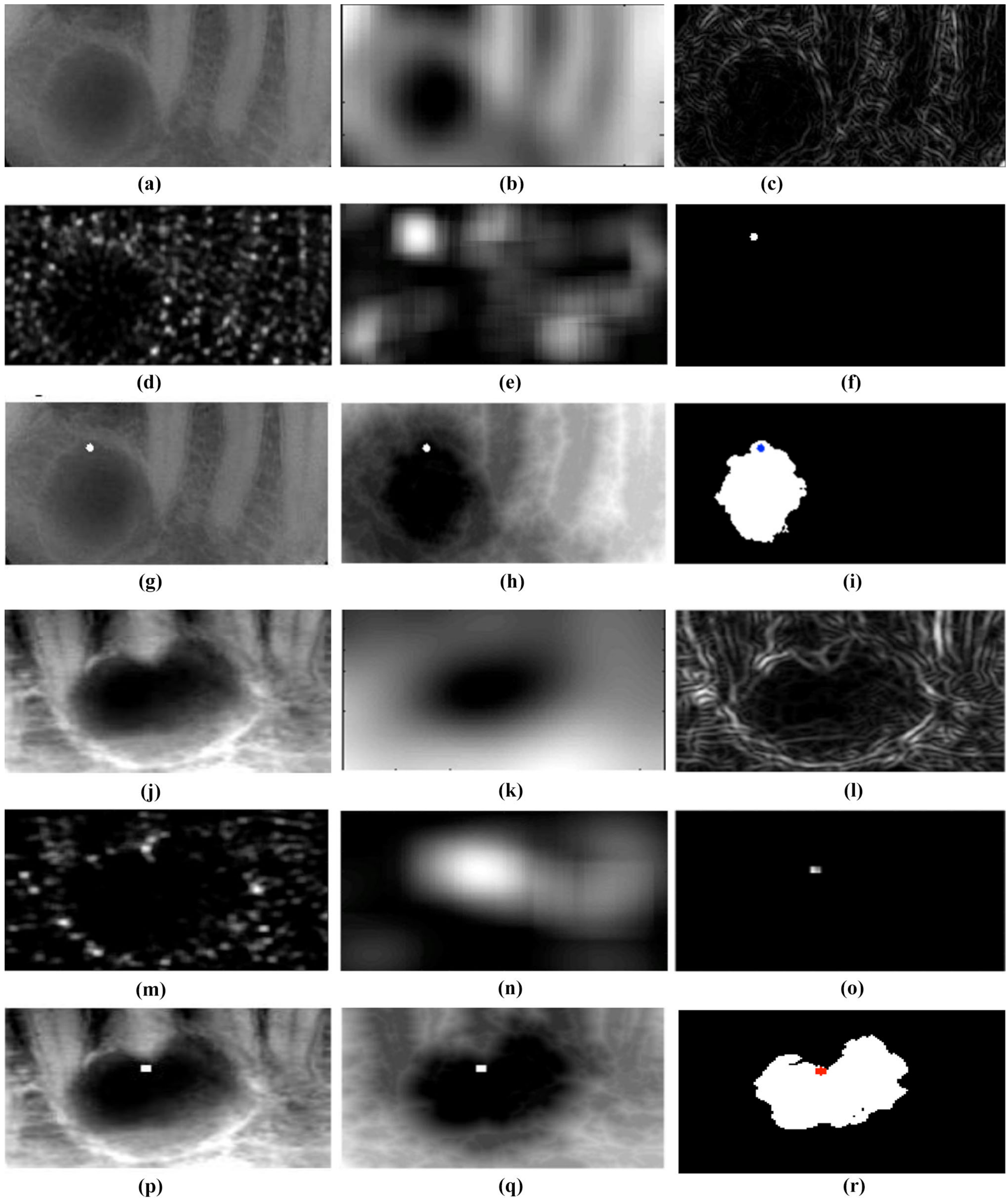

Fig. 8 Detection of dental cyst using isophote curvature and fast marching method. **a** Original image 1, **b** Gaussian blurring, **c** measure of curvedness, **d** isophotes, **e** mapped image after blurring, **f** maximum IsoCenter, **g** initial point selected by MIC, **h** geodesic distance of FMM, **i** extracted cyst by FMM, **j** original image 2, **k** Gaussian blurring, **l** measure of curvedness, **m** isophotes, **n** mapped image after blurring, **o** maximum isocenter, **p** initial point selected by MIC, **q** geodesic distance of FMM, **r** extracted cyst by FMM

region very effectively where the seed point originated by maximum isocenter (MIC) of Isophote curvature. The output shows that how the cyst is segmented from the periapical image using fast marching method (FMM) based on differences in gray level intensity as compared to the seed locations (Fig. 8).

5 Performance evaluation of proposed method

5.1 Accuracy

The accuracy can be calculated as

$$Accuracy = \frac{(\mathrm{TP} + \mathrm{TN})}{(\mathrm{TP} + \mathrm{TN} + \mathrm{FP} + \mathrm{FN})}$$

TP is the true positive; FP is the false positive; TN is the true negative; FN is the false negative

5.2 Geodesic distance

The spatial characteristic modeling is complicated along a surface than in imaging plane. Because of the sampling used is irregular for mesh representation. This is the unique situation occurs in the delineation of the non-Euclidean domain. The distance between two points on the surface connected by a geodesic or length minimizing curve is called "geodesic distance" [20,21] shown in Fig. 9.

5.3 Dice similarity index

The dice similarity index is used to measure the overlapped similarity between the ground truth and manual segmented area A_{MS} and the automated segmented regions A_{AS}.

$$D = \frac{2\,|A_{MS} \cap A_{AS}|}{|A_{MS}| + |A_{AS}|}$$

where $|A_{MS} \cap A_{AS}|$ represents the overlapping region between the manually segmented cystic region and the segmented cystic region by the proposed method. If the value of dice coefficient is nearer to the value one means that the segmented output is closer to ground truth image.

6 Results and discussion

The dental X-ray images are collected from Maoris Dental Hospital, Dindigul. Figure 8 shows the sample outputs in which (a)–(i) demonstrate the intermediate results for sample image 1, and (j)–(r) shows the output of sample image

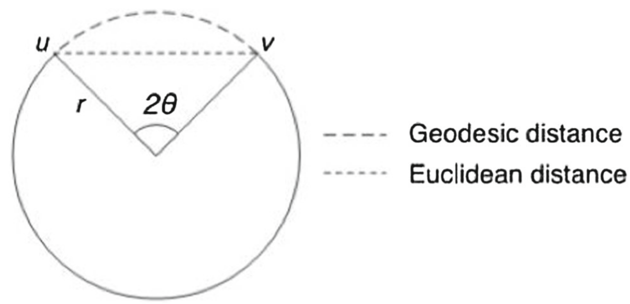

Fig. 9 Geodesic distance

Table 3 Mean run time and seed point location by the proposed method

Image	Seed point location (C,R)	Size	Mean run time
			Auto seed selection using MIC (sec)
Image1	60,24	113 X,246	3.31
Image2	27,77	155 X,136	2.78
Image3	68,45	118 X,156	2.32

2. The proposed two stages, hybrid, the automated method extracts all size of the cyst and in any location mainly radicular and follicular cyst. The irregular boundary also extracted by means of the proposed method, without any intervention of the human. It extracts the cyst region from the complex structure of dental X-rays from the uneven distribution of cyst.

From Table 3 the mean execution time for three images are calculated using proposed approach and other segmentation methods. The performance metrics outcomes are given in Table 4, which shows that the proposed method is faster than the other methods.

In Fig. 11, the live wire segmentation is taken as ground truth for the input image [18,21].The comparison of multilevel histogram based thresholding [22], watershed [18,23], and Active contour [19,24] methods with the proposed approach are carried out. The dentist verified the extracted results of manual cropping through the live wire. However, it requires more trained medical experts or manual operator. The multilevel thresholding requires the number of the threshold for segmentation, and Watershed algorithm results in an under segmentation that is over-segmentation. The initial parameters have to be set inactive contour-based segmentation. When compared to other methods, the proposed method works well for all cyst images and no over-segmentation. There is no need for parameter selection, the selection of a number of thresholds and avoids human intervention except the region of interest selection. This advanced method is suitable for periapical and bitewing view of the dental X-ray images. Figure 10b shows the geodesic out-

Table 4 Performance metrics. (1) Livewire, (2) Multi-level thresholding, (3) Watershed algorithm, (4) Active contour (200 iterations) and (5) proposed the method

Method	Mean run time (s)			DICE similarity index			MAD			Accuracy			Mean (cystic region)
	I1	I2	I3	I1	I2	I3	I1	I2	I3	I1	I2	I3	
1.	55.02	42.34	47.53	Ground truth			8.78	8.86	8.54	Ground truth			66.44
2.	9.73	8.01	7.41	0.57	0.52	0.67	8.23	8.10	8.20	0.80	0.86	0,89	71.87
3.	3.33	2.81	2.40	0.71	0.74	0.65	9.78	9.23	9.38	0.87	0.81	0.85	71.23
4.	7.99	6.61	6.35	0.79	0.76	0.78	7.83	7.56	7.69	0.94	0.90	0.93	61.99
5.	3.31	2.78	2.32	0.89	0.89	0.88	5.73	5.57	5.02	0.95	0.94	0.92	63.21

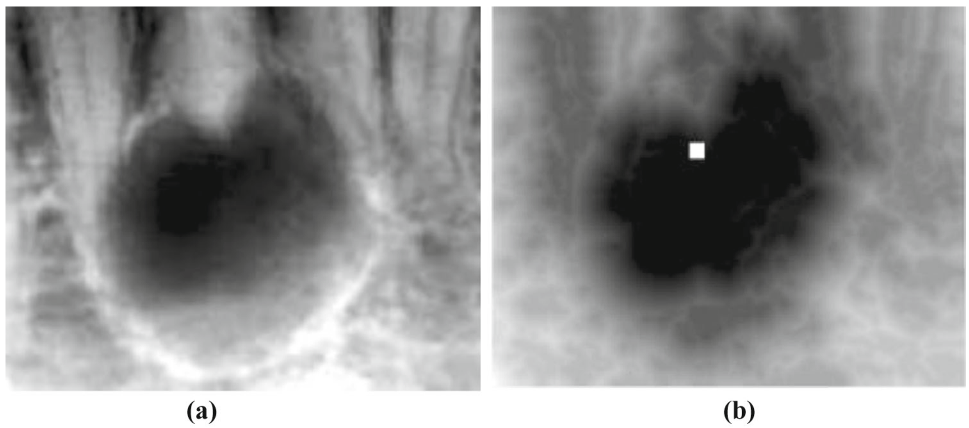

Fig. 10 Result of the geodesic distance of cyst image. **a** Original image and **b** geodesic distance of the original image

put. It is the shortest path between two vertices in a graph and called as graph geodesic, and connecting the edges most shortly. Figure 11h gives the overlapped region between the result of the proposed method and the ground-truth.

In Table 4, the performance metrics are calculated and tabulated for three sample images. The parameters are mean run time. DICE similarity index, mean absolute deviation, accuracy, and Mean of the extracted cystic region. From the metrics, it proves that the method faster than other, the average dice index of 0.89 and it shows that there is a strong correlation between the cystic regions extracted by a medical expert and the cystic region segmented by the proposed method. The maximum segmentation accuracy achieved is 95%.

7 Conclusion

Nowadays manual segmentation or manual selection of parameters for segmentation will become time-consuming, laborious, and requires a more trained operator. Therefore, it is necessary to develop fully automated image segmentation suitable for every problem to obtain a precise and meaningful result in medical application. The proposed method introduced two stages, hybrid, fast, fully automated one to segment the cyst in dental X-ray images. For that hybrid approach, both feature-based Isophote curvature and model-based fast marching method (FMM) are combined. At first, the feature based Isophote curvature extracted the maximum IsoCenter from the 'input cystic image to locate the cystic region from the complex structures of teeth. That MIC used as an initial point for fast marching method. The FMM is a modified algorithm of shortest path algorithm used for image segmentation. This proposed hybrid method extracts the cyst very efficiently even though they are in the uneven structure. The hybrid approach works well and segments the cyst in all size and location. Therefore, this method is fully automated, fast, and efficient. The comparison of results shows that this hybrid method works better than other methods and it proves that there is no over-segmentation. Only the cystic region is extracted exactly with distinct boundaries. This automatic cyst boundary extraction will assist the doctors in further processing like severity measure, surgery of cyst successively. The advantages attained by the proposed methodology are (1) there is a strong line of separation between the cystic region and other parts of the teeth. (2) It is fully automatic so no parameter initialization (3) The complicated cystic region also extracted (4) It extracts any cyst, which varies in size. This method eliminates the disadvantages of time-consuming, manual segmentation and the need for trained radiologist.

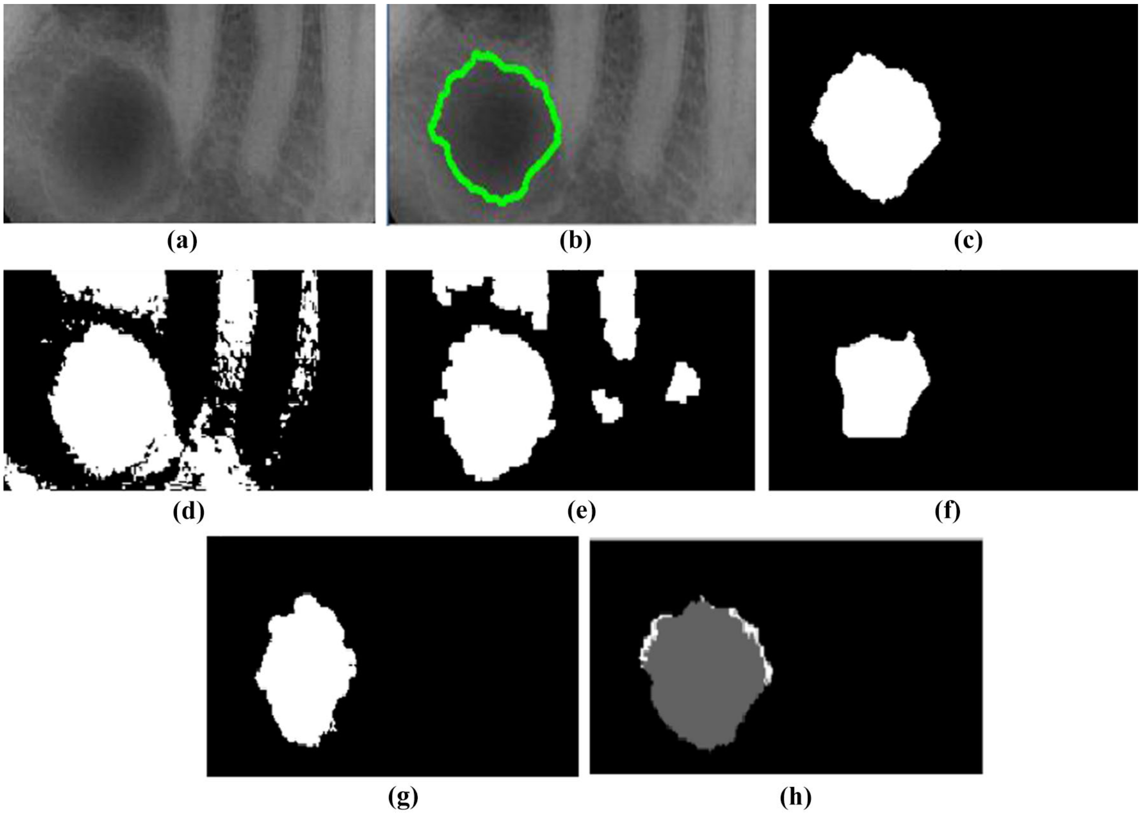

Fig. 11 Comparison of the proposed method with other methods. **a** the original image, **b** live-wire drew, **c** extracted cyst region by live-wire (ground truth), **d** multi-level thresholding, **e** watershed output, **f** active contour output, **g** the result of the proposed approach, and **h** dice similarity calculation

Acknowledgements We want to thank Dr.P. Senthilkumar, MDS, Maxillofacial Surgery, Maeoris Dental Hospital Dindigul for providing the medical image data and interpretation for the analysis and we thank Dr. N. Dinakaran M.S. Head of the Department—ENT, Government Rajaji Hospital, Madurai for his full support in doing this work.

References

1. Katsumata, A., Fujita, H.: Progress of computer-aided detection/diagnosis (CAD) in dentistry CAD in dentistry. Jpn. Dent. Sci. Rev. **50**(3), 63–68 (2014)
2. Tsiklakis, K., Damaskos, S., Kalyvas, D., Nicopoulou-Karayianni, K., Van der Stelt, P.F.: The use of digital subtraction radiography to evaluate bone healing after surgical removal of radicular cysts. Oral Radiol. **21**(2), 56–61 (2005)
3. Chodorowski, A., Mattsson, U., Langille, M., Hamarneh, G.: Color lesion boundary detection using live wire. Int. Soc. Optics Photon. Med. Imaging **5747**, 1589–1596 (2005)
4. Li, S., Fevens, T., Krzyżak, A., Jin, C., Li, S.: Semi-automatic computer-aided lesion detection in dental X-rays using variational level set. Pattern Recogn. **40**(10), 2861–2873 (2007)
5. Alazab, M., Islam, M., Venkatraman, S.: Towards automatic image segmentation using optimised region growing technique. In: Proceedings of the Australasian Joint Conference on Artificial Intelligence, Springer, pp. 131–139 (2009)
6. Mikulka, J., Gescheidtova, E., Kabrda, M., PEŘINA, V.: Classification of jaw bone cysts and necrosis via the processing of orthopantomograms. Radioengineering **22**(1), 115 (2013)
7. Hamarneh, G., Chodorowski, A., Gustavsson, T.: Active contour models: application to oral lesion detection in color images. In: Proceedings of the 2000 IEEE International Conference on Systems, Man, and Cybernetics, vol. 4, IEEE, pp. 2458–2463 (2000)
8. Lin, P.L., Huang, P.Y., Huang, P.W.: An automatic lesion detection method for dental x-ray images by segmentation using variational level set. In: Proceedings of the 2012 International Conference on Machine Learning and Cybernetics (ICMLC), vol. 5, IEEE, pp. 1821–1825 (2012)
9. Birdal, R.G., Gumus, E., Sertbas, A., Birdal, I.S.: Automated lesion detection in panoramic dental radiographs. Oral Radiol. **32**(2), 111–118 (2016)
10. Abdolali, F., Zoroofi, R.A., Otake, Y., Sato, Y.: Automatic segmentation of maxillofacial cysts in cone beam CT images. Comput. Biol. Med. **72**, 108–119 (2016)
11. Banumathi, A., Kannammal, A., Arthee, R., Raju, S., Abhaikumar, V.: Automated diagnosis and severity measurement of cysts in dental X-ray images using the neural network. Biomed. Fuzzy. Hum. Sci. **11**(1), 15–19 (2006)
12. Berdouses, E.D., Koutsouri, G.D., Tripoliti, E.E., Matsopoulos, G.K., Oulis, C.J., Fotiadis, D.I.: A computer-aided automated methodology for the detection and classification of occlusal caries from photographic color images. Comput. Biol. Med. **62**, 119–135 (2015)
13. Zhu, H., Zhuang, Z., Zhou, J., Zhang, F., Wang, X., Wu, Y.: Segmentation of liver cyst in ultrasound image based on adaptive threshold algorithm and particle swarm optimization. Multimed. Tools Appl. **76**(6), 8951–8968 (2017)

14. Zhu, H., Sheng, J., Zhang, F., Zhou, J., Wang, J.: Improved maximally stable extremal regions based method for the segmentation of ultrasonic liver images. Multimed. Tools Appl. **75**(18), 10979–10997 (2016)
15. Valenti, R., Gevers, T., Accurate eye center location and tracking using isophote curvature, In: Proceedings of the IEEE Conference on Computer Vision and Pattern Recognition: CVPR 2008, IEEE 2008, pp. 1–8 (2008)
16. Valenti, R., Gevers, T.: Accurate eye center location through invariant isocentric patterns. IEEE Trans. Pattern Anal. Mach. Intell. **34**(9), 1785–1798 (2012)
17. Sethian, J.A.: A fast marching level set method for monotonically advancing fronts. Proc. Nat. Acad. Sci. **93**(4), 1591–1595 (1996)
18. Meyer, F.: Topographic distance and watershed lines. Sig. Process. **38**(1), 113–125 (1994)
19. Chen, G., Gu, L., Qian, L., Xu, J.: An improved level set for liver segmentation and perfusion analysis in MRIs. IEEE Trans. Inf. Technol. Biomed. **13**(1), 94–103 (2009)
20. Barrett, W.A., Mortensen, E.N.: Interactive live-wire boundary extraction. Med. Image Anal. **1**(4), 331–341 (1997)
21. Mortensen, E.N., Barrett, W.A.: Interactive segmentation with intelligent scissors. Graph. Models Image Process. **60**(5), 349–384 (1998)
22. Papamarkos, N., Gatos, B.: A new approach for multilevel threshold selection. CVGIP **56**(5), 357–370 (1994)
23. Kim, S.: An o(n) level set method for Eikonal equations. SIAM J. Sci. Comput. **22**(6), 2178–2193 (2001)
24. Chan, T.F., Vese, L.A.: Active contours without edges. IEEE Trans. Image Process. **10**(2), 266–277 (2001)

R. Karthika Devi completed her B.E. during the year 1998 and received M.E. (Communication Systems) from Thiagarajar College of Engineering, Madurai, in the year of 2002 and Pursuing Ph.D. in the research area of Medical Image Processing. Now working as Associate Professor in Sethu Institute of Technology.

A. Banumathi completed B.E. during the year 1984 and received M.E. (Communication Systems) from Thiagarajar College of Engineering, Madurai, and received Ph.D. in the area of Medical Image Processing from Madurai Kamaraj University during the year 2009. Her research area includes medical imaging especially in dental imaging. Her research publications comprise publications in refereed journal and various national and international conferences. One of her research work is published as international patent and another has been granted. She is the receipt of New Invention award. She is working on a research project supported and funded by the University Grants Commission (UGC), New Delhi, India.

G. Ulaganathan completed B.D.S. during the year 1984 from Madras Dental College and received M.D.S during the year 2006 from Raja Muthiah Dental College, Chidambaram. His area of specialty is Oral and Maxillofacial Surgery. His research interest includes the area of facial trauma management, facial cyst and tumor surgeries, oral pathology, dental implantology, and T.M joint surgery.